Effect of microstructure on diffusion of copper in TiN films

A. Gupta,[a] H. Wang, and A. Kvit
Department of Materials Science and Engineering and NSF Center for Advanced Materials and Smart Structures, North Carolina State University, Raleigh, North Carolina 27695-7916.

G. Duscher
Department of Materials Science and Engineering and NSF Center for Advanced Materials and Smart Structures, North Carolina State University, Raleigh, North Carolina 27695-7916 and Solid State Division, Oak Ridge National Laboratory, Oak Ridge, Tennessee 37831

J. Narayan
Department of Materials Science and Engineering and NSF Center for Advanced Materials and Smart Structures, North Carolina State University, Raleigh, North Carolina 27695-7916.

(Received 28 October 2002; accepted 18 February 2003)

We investigated the effect of the microstructure of TiN films on the diffusion behavior of Cu. Cu/TiN films were synthesized on Si(100) substrate by the pulsed laser deposition (PLD) technique. Three different microstructures of TiN were achieved by growing the films at different substrate temperatures, where higher deposition temperatures ($\sim 650\,^{\circ}\mathrm{C}$) led to epitaxial growth by the mechanism of domain matching epitaxy and lower temperature depositions resulted in polycrystalline and nanocrystalline TiN films. These structures were characterized using x-ray diffraction and high-resolution transmission electron microscopy. Cu was deposited *in situ* on the samples with three different microstructures of TiN films on Si(100) by PLD. All three samples were simultaneously annealed at 500 °C for 30 min in high vacuum to study the effect of diffusion characteristics of Cu as a function of microstructure of the TiN films. Secondary ion mass spectroscopy, *Z*-contrast imaging and electron energy-loss spectroscopy were used to understand the diffusion mechanisms and rationalize results in different microstructures. © *2003 American Institute of Physics.* [DOI: 10.1063/1.1566472]

I. INTRODUCTION

Cu has attracted considerable attention as an interconnect layer because of its low resistivity (1.67 $\mu\Omega$ cm for bulk) and its high reliability against electromigration and stress migration.[1,2] However, the high diffusivity of Cu in Si ($D \approx 10^{-8}\,\mathrm{cm}^2/\mathrm{s}$) makes it a fatal impurity, which reduces the minority carrier lifetime in devices.[2] Therefore a thin diffusion barrier preventing Cu diffusion is required to integrate Cu as an interconnect layer. TiN has been widely investigated as a diffusion barrier layer for metalization.[3] Among the diffusion barriers like Ta, TaN, and WN, TiN offers some advantages like low resistivity, low impurity contamination, good Cu film adhesion and well developed processing techniques.[4–6] The microstructure of TiN is the most important characteristic that affects the diffusion behavior of Cu in TiN films.[7–9] Polycrystalline films contain grain boundaries, which provide fast diffusion paths for metals[10] and increase the electrical resistivity by grain boundary scattering. Epitaxial layers do not have grain boundaries and therefore eliminate the fast diffusion paths and also enhance electrical conductivity of the film.

The effect of microstructure on diffusion can be analyzed by growing TiN films with different microstructures such as single crystalline, polycrystalline and nanocrystalline structures, followed by deposition of Cu on each sample, and annealing the three samples simultaneously in high vacuum above the breakdown temperature. *Z*-contrast imaging in the scanning transmission electron microscopy (TEM) which gives different contrast of the element due to its different atomic number (Z^2 dependence) and electron energy-loss spectroscopy (EELS) which allows compositional analysis by detecting the characteristic energy loss of the electron of the particular element, act as powerful tools to trace the diffusion profile of Cu.

II. EXPERIMENT

Silicon (100) substrates were cleaned to remove the surface oxide layer using a 49% HF solution. Uniform films of TiN were deposited on Si(100) by pulsed laser deposition (PLD) followed by *in situ* PLD deposition of uniform Cu layer on the TiN/Si substrate. The films were deposited inside a stainless-steel vacuum system evacuated by a turbomolecular pump to a base pressure of 1×10^{-7} Torr. A KrF excimer laser ($\lambda = 248$ nm, $\tau \sim 25$ ns) was used for the ablation of TiN and Cu targets. The stoichiometric hot pressed TiN and high purity Cu targets, mounted on a rotating polygon, were ablated at an energy density of $3.0-3.5\,\mathrm{J/cm}^2$. The films were deposited at a laser repetition rate of 10 Hz for 10 min each. TiN films were deposited at three different temperatures ~ 25, 450, and 600 °C to achieve different microstructures. Deposition of Cu was done at room temperature because higher substrate temperature leads to Stranski–

[a]Author to whom correspondence should be addressed; electronic mail: agupta@unity.ncsu.edu

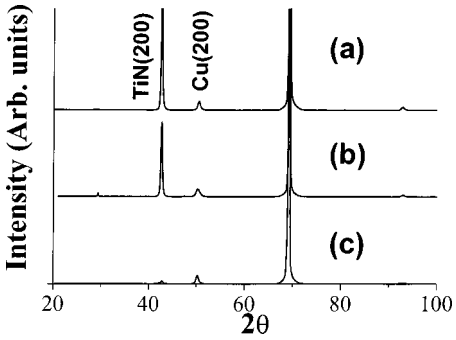

FIG. 1. X-ray diffraction pattern for Cu(100)/TiN(100)/Si(100) films with (a) single crystalline TiN films, (b) polycrystalline TiN films, and (c) nanocrystalline TiN films.

Krastanov island growth of Cu on TiN/Si substrate.[11] Then the deposited films were analyzed by x-ray diffraction using a Rigaku diffractometer equipped with Cu K_α source operating at a power as high as 5 KW. The nature of epitaxy in these films was also studied using cross-section samples in a 200 keV JEOL 2010F high-resolution transmission electron microscope with point-to-point resolution of 1.8 Å. In this study, TiN barrier layers of ~120 nm thickness and uniform Cu layer of ~20 nm were deposited at optimized conditions. These samples were annealed at a base pressure of 1×10^{-6} Torr at 500 °C for 30 min. All the annealed and unannealed samples were studied by secondary ion mass spectroscopy (SIMS), *Z*-contrast imaging and EELS to study the effect of the microstructure of TiN films on the diffusion behavior of Cu. SIMS analysis was performed on a CAMECA IMS-6f using O_2^+ primary beam with impact energy of 1.25 KeV and mass resolution of 4400. Secondary ions were detected from a 60-μm-diam region in the center of a 300 μm×300 μm raster.

III. RESULTS AND DISCUSSION

The pulsed laser deposition (PLD) lends itself to low substrate temperature processing because the average energy of particles in the laser-evaporated species is considerably higher (100–1000 kT) compared to the thermal evaporation energy (kT). This extra energy is utilized in recrystallization of films.[12] By reducing the substrate temperature the energy provided for recrystallization is reduced and the films lose their texture and become polycrystalline at ~450 °C and nanocrystalline at ~25 °C.[13] We have reported the growth of epitaxial layers of TiN on Si(100) by domain matching epitaxy above 600 °C by PLD.[14] The domain matching epitaxy mechanism involves the matching of four unit cells of TiN with three unit cells of silicon across the interface for epitaxial relationship.[15] The electrical resistivity of single-crystal TiN films (~15 $\mu\Omega$ cm) was close to that of $TiSi_2$ (~C −54) polycrystalline films, thus making these films attractive for contact metallurgy as well as diffusion barrier.

Figure 1 compares the x-ray diffraction pattern of the different TiN films on (100) silicon substrates. The patterns in Figs. 1(a) and 1(b) contain (200) and (400) TiN reflections along with (400) Si reflections indicating that the growth of TiN films is highly textured with the silicon substrate along the (100) axis. The x-ray diffraction of TiN films in Fig. 1(a) shows an intense sharp peak of (200) oriented single crystalline TiN films indicating a highly textured nature of the film. Lowering the temperature degrades the crystal quality and lowers the (200) peak of polycrystalline TiN films as seen in the Fig. 1(b). The nanocrystalline TiN films in Fig. 1(c) lose their texture and get randomly oriented. Figure 2 compares the selected-area electron-diffraction patterns of the films containing Cu and TiN and Si taken from (110) cross section TEM specimen. Electron diffraction together with the x-ray diffraction studies give us a three-dimensional orientation relationship. TiN and Si diffraction spots for single crystalline TiN films shown in the Fig. 2(a) align with respect to each other, while the fourth order diffraction spots of TiN match within 4% with the third order spots of the Si substrate. A simulated diffraction pattern of Cu, TiN, and Si is shown in Fig. 2(b) to compare with the actual diffraction pattern shown in Fig. 2(a). These patterns clearly establish cube-on-cube alignment between the TiN layer and the Si substrate. The selected-area diffraction patterns of the polycrystalline TiN films in Fig. 2(c) exhibits arcs which indicate a lower degree of epitaxy. The diffraction pattern turns into continuous rings corresponding to (111), (200), and (220) planes of the NaCl structure for the randomly oriented nanocrystalline TiN film shown in Fig. 2(d). The ⟨100⟩ textured films should contain ⟨200⟩, ⟨220⟩, and ⟨400⟩ rings only. In order to study the in-plane alignment of the TiN films with respect to the Si substrate and their epitaxial nature, cross section specimens were studied using a TEM (JEOL 2010F) instrument. Figure 3(a) shows the high-resolution micrograph of the interface between the single crystalline TiN and (100) Si substrate, which was found to be very smooth and free from any perceptible interdiffusion.

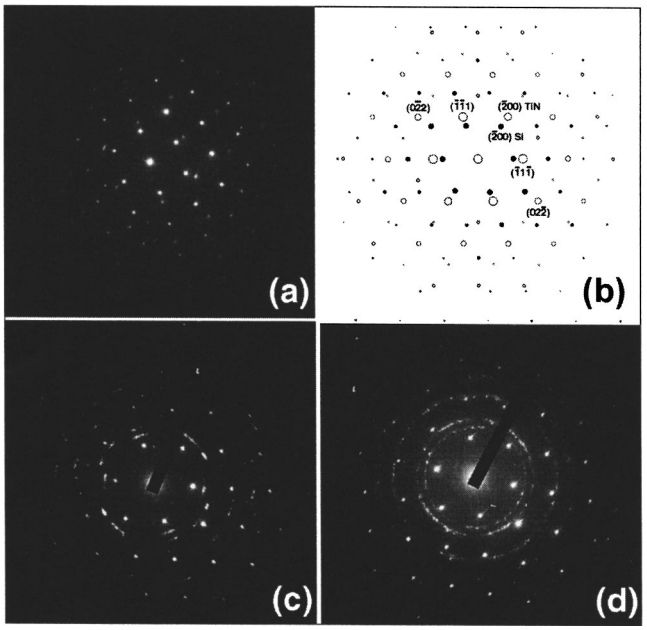

FIG. 2. Electron diffraction pattern of TiN films grown at different temperatures: (a) single crystalline TiN films (~650 °C), (b) simulated pattern of TiN, (c) polycrystalline TiN films (~450 °C), and (d) nanocrystalline TiN films (~25 °C) showing the presence of rings with (111), (200), and (220) orientations.

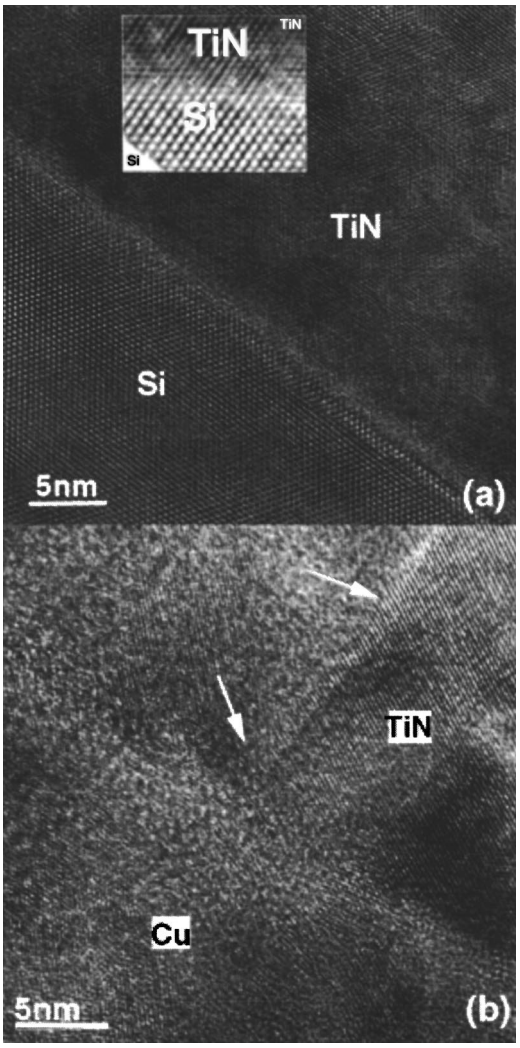

FIG. 3. High-resolution TEM images for single crystalline TiN film sample with (a) Si/TiN interface. The inset picture is a magnified TiN/Si interface showing misfit dislocation. (b) The Cu/TiN interface showing a low angle grain boundary (marked by an arrow).

The (111) planes in silicon with 0.314 nm spacing are aligned with (111) TiN planes with 0.244 nm spacing. The lattice constant of TiN films was determined to be 0.422 nm. The dislocations associated with extra half planes terminating at the interface were observed at the interface shown in the inset of Fig. 3(a). These dislocations relieve the lattice misfit strain between the TiN layer and the Si substrate by domain matching epitaxy.[15] Although the film is epitaxial, it contains a high density of dislocations at the interface. Figure 3(b) shows a good adhesion of Cu layer on the single crystal TiN films, which is an important issue in the integrated circuits. It also shows a low angle grain boundary, which could act as a fast diffusion path for Cu. Low magnification TEM image of the polycrystalline TiN films shows a partial columnar growth shown in Fig. 4. The bright field and dark field TEM images of nanocrystalline TiN films shown in Figs. 5(a) and 5(b), respectively, show nanocrystalline TiN films with random orientations of the grains with average grain size of around 8 nm.

After attaining the three desired microstructures of TiN films, the samples were annealed at 500 °C for 30 min to

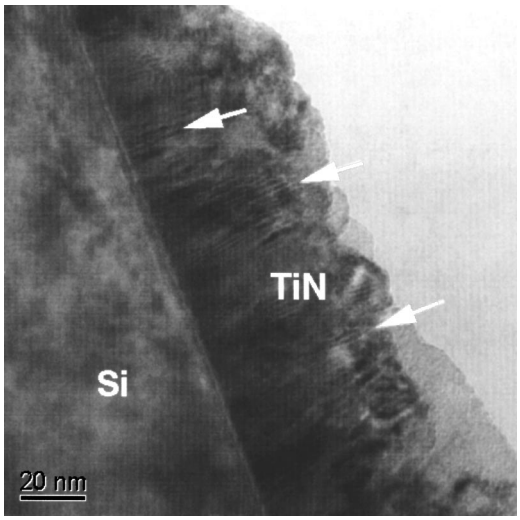

FIG. 4. TEM image of polycrystalline TiN films with the columnar structure indicated by the arrows directly connecting the overlayer with the substrate.

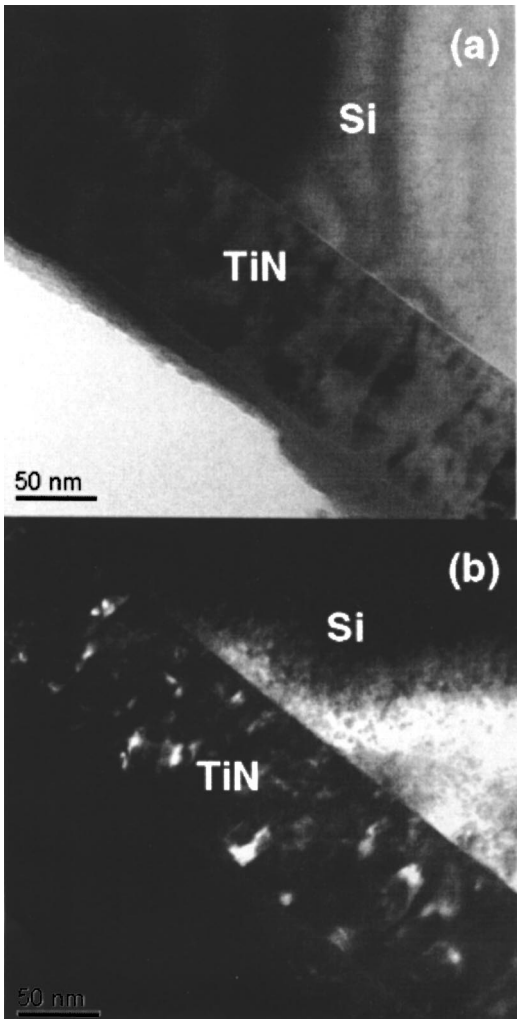

FIG. 5. (a) Bright field, and (b) dark field TEM images of nanocrystalline TiN film sample confirming the nanocrystalline TiN films with the average grain size of 8 nm.

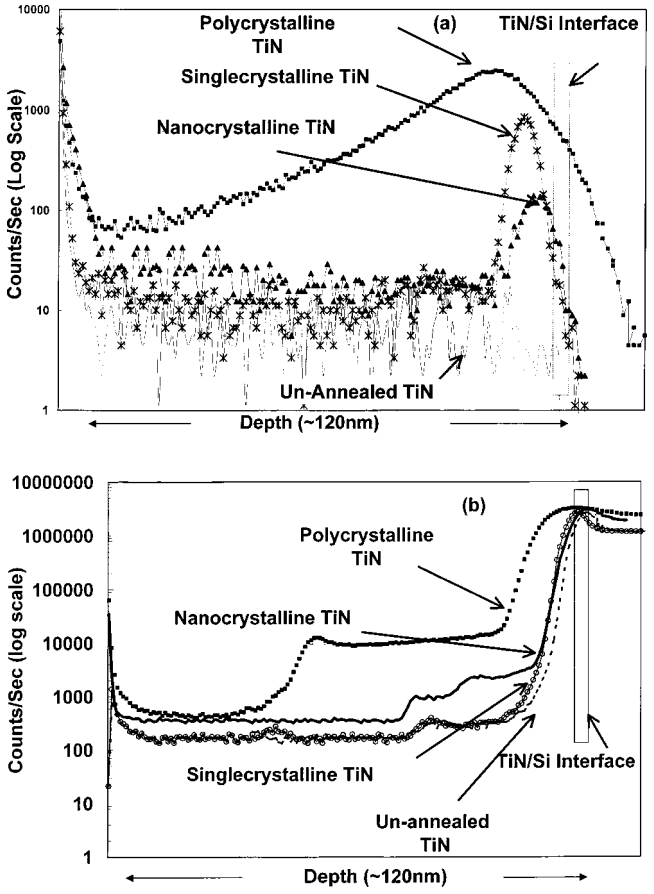

FIG. 6. SIMS profiles comparing the diffusion profile of (a) Cu, and (b) Si in all the three microstructures of TiN samples annealed at 500 °C for 30 min. The box indicates the approximate location of the interface for the three samples. The depth of the TiN films is around (~120 nm). Polycrystalline TiN showed the maximum diffusion of Cu and Si.

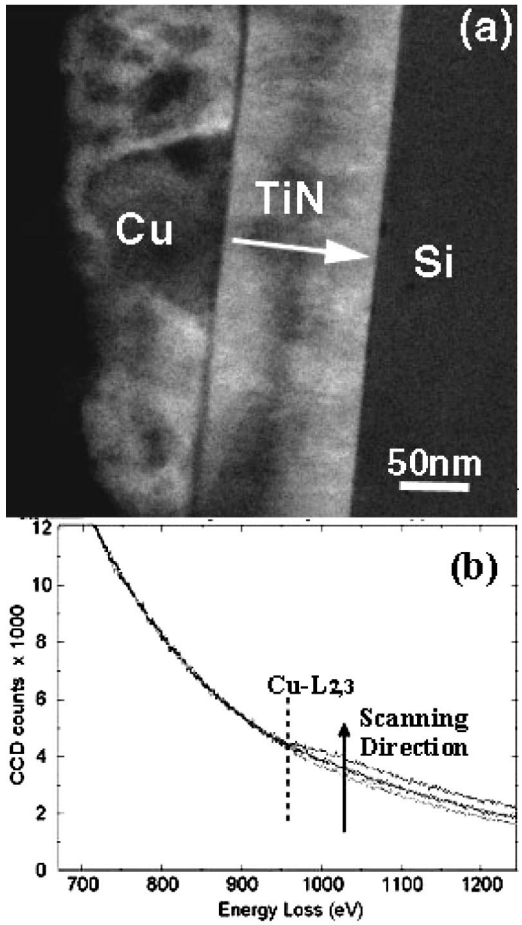

FIG. 7. (a) *Z*-contrast image, and (b) EELS spectrum for the annealed single crystalline TiN film sample. Scanning direction of the probe formed for EELS is shown by the arrow.

diffuse Cu into TiN films. The presence of undiffused Cu films on TiN could overshadow the signal from the diffused Cu in TiN films for the SIMS experiment. To prevent this the Cu films on top of TiN films were removed after annealing with an etching agent consisting of NH_4OH (20 ml); H_2O_2 (20 ml), H_2O (10 ml). To compare the effect of the microstructure on the diffusion of Cu, SIMS profiles for all three microstructures of TiN samples after annealing are shown in Fig. 6(a) along with the unannealed sample. For the diffusion of Si in TiN films from the substrate, SIMS profiles are shown in Fig. 6(b). Interestingly, the diffusion profile of the Cu is not the usual Gaussian profile, but it increases with depth with a maximum just before the interface. The dislocations present at the TiN/Si interface might cause Cu segregation or the interstitials and vacancies in TiN films might alter the kinetics of the diffusion process.[16] In SIMS experiment, a sharp increase in Cu profile and the step profile of Si indicate a phase formation. Copper silicide is usually observed in similar diffusion experiments.[4] Single crystalline and nanocrystalline TiN films show significantly less Cu diffusion than polycrystalline TiN films. The pseudo columnar growth of polycrystalline films containing grain boundaries, which connect the over layers with the substrate, might serve as a fast diffusion path for metals. Activation energy for diffusion along grain boundaries is less than half of activation energy for single crystalline TiN films.[10,17] Single crystal TiN films have few low angle grain boundaries shown in Fig. 3(b) connecting the overlayers, which could act as a direct diffusion path for Cu leading to some diffusion of Cu. The high density of dislocation at the interface acts probably as a segregation site for Cu. Interestingly, we see much less diffusion of Cu in nanocrystalline TiN films compared to single crystalline TiN films. Nanocrystalline TiN has equiaxed grain boundaries and the diffusivity paths associated are effectively much longer, which could have effectively led to less diffusion of Cu. Also the various atomic structures (various tilt and twist components) of the grain boundaries are assumed to promote different diffusivity and thus could cause the differences in the diffusion profiles. Theoretically, special orientations corresponding to a high density of coincidence sites may give highly ordered grain boundary (GB) structures showing minima of GB diffusivity. It has been seen that accurate measurements on Cu bicrystals with symmetrical tilt GBs around the Sigma $=5(310)[001]$ orientation have shown a very narrow minimum for both Au impurity diffusion (weak segregation) and Cu self-diffusion.[18]

Z-contrast imaging together with EELS is a powerful technique to analyze diffusion with high accuracy.[19] Figure 7(a) shows the *Z*-contrast image of annealed sample of Cu/TiN (single crystalline)/Si where the probe formed by the

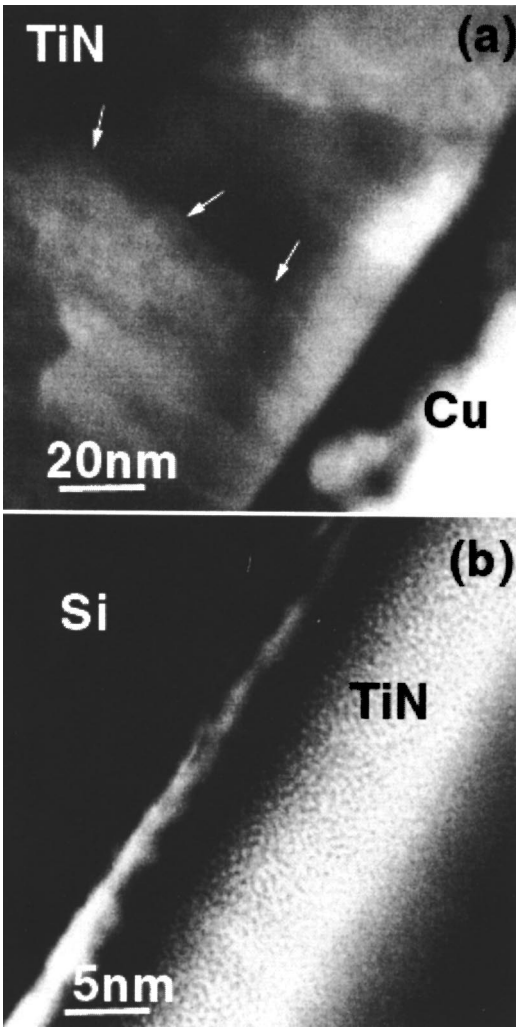

FIG. 8. Z-contrast image of the annealed polycrystalline TiN sample showing (a) grain boundaries in TiN films, and (b) bright layer near the TiN/Si interface. Bright layer is due to the excess concentration of the diffused elements.

electron beam was scanned across the sample as indicated by the arrow to detect the Cu signal with EELS as shown in Fig. 7(b), where the Cu$-L_3$ edge onset corresponds to 931 eV. We see an increase in the Cu signal as we scan across the TiN films and the maximum in the signal at the TiN/Si interface, which is consistent with the SIMS results. *Z*-contrast images of annealed polycrystalline sample show grain boundaries in Fig. 8(a) and Fig. 8(b) shows a bright layer in the TiN films, which we do not see in the unannealed sample. The brightness is attributed to the presence of a significant concentration of Cu and Si corresponding to the SIMS results. Future studies will use the techniques to detect the presence of Cu in different grain boundaries, perform a compositional analysis of the diffused elements along with SIMS experiments, and possibly reveal the origin of the anomalous diffusion behavior of Cu in TiN films.

IV. CONCLUSIONS

We have produced three different microstructures such as nanocrystalline, polycrystalline, and single crystalline TiN films by pulsed laser deposition by varying the substrate temperature. X-ray diffraction and high-resolution transmission electron microscopy techniques were used to analyze the microstructures of these films. The as-deposited samples of Cu/TiN/Si with different microstructures of TiN films were annealed at 500 °C for 30 min. Secondary ion mass spectroscopy along with *Z*-contrast imaging and electron energy loss spectroscopy were used to study the diffusion behavior of Cu in TiN films. Polycrystalline samples showed the maximum diffusion of Cu in TiN films compared with single crystalline and nanocrystalline TiN films due to the columnar grains proving a direct diffusion path. Few low angle grain boundaries present in the highly textured single crystalline TiN films sample also provided a direct diffusion path between, also leading to some diffusion of Cu. Nanocrystalline TiN films showed the least diffusion. It could be due to the different microstructure (not columnar) and effectively much longer diffusion path for nano size grains or due to different diffusivity at different grain boundaries with differences in the tilt and twist angles of the boundaries. In summary, we find that nanocrystalline TiN films are promising diffusion barriers.

ACKNOWLEDGMENT

The authors are pleased to acknowledge the NSF support under the center of Advanced Materials and Smart Structures.

[1] J. O. Olowolafe, J. Li, and J. W. Mayer, J. Appl. Phys. **68**, 6207 (1990).
[2] P. Murarka, Mater. Sci. Eng., R. **19**, 87 (2000).
[3] A. E. Kaloyeros and E. Eisenbraun, Annu. Rev. Mater. Res. **30**, 363 (2000).
[4] C. Carbal, Jr., C. Lavoie, J. M. E. Harper, and J. Jordan-Sweet, Thin Solid Films **397**, 194 (2001).
[5] C. L. Lin, P. S. Chen, and M. C. Chen, J. Vac. Sci. Technol. B **20**, 1111 (2002).
[6] S. K. Rha, S. Y. Lee, W. J. Lee, Y. S. H. Wang, C. O. Park, D. W. Kim, Y. S. Lee, and C. N. Whang, J. Vac. Sci. Technol. B **16**, 2019 (1998).
[7] J. M. E. Harper and K. P. Rodbell, J. Vac. Sci. Technol. B **15**, 763 (1997).
[8] T. Kouno, H. Niwa, and M. Yamada, J. Electrochem. Soc. **145**, 763 (1998).
[9] K. C. Park, K. B. Kim, I. J. M. M. Raaijmakers, and K. Ngan, J. Appl. Phys. **80**, 5674 (1996).
[10] M. B. Chamberline, Thin Solid Films **91**, 155 (1982).
[11] R. D. Vispute, R. Chowdhury, P. Tiwari, and J. Narayan, Appl. Phys. Lett. **65**, 2565 (1994).
[12] R. K. Singh and J. Narayan, Phy. Rev. 41.
[13] H. Wang, A. Sharma, A. Kvit, Q. Wei, X. Zhang, C. C. Koch, and J. Narayan, J. Mater. Res. **16**, 2733 (2001).
[14] J. Narayan, P. Tiwari, X. Chen, J. Singh, R. Chowdhury, and T. Zheleva, Appl. Phys. Lett. **61**, 1290 (1992).
[15] J. Narayan, U.S. Patent No. 5,406,123.
[16] S. P. Murarka, I. V. Verner, and R. J. Gutmann, *Copper-Fundamental Mechanisms from Microelectronic Applications* (Wiley, New York, 2000), pp. 49-54.
[17] K. Y. Lim, Y. S. Lee, Y. D. Chung, I. W. Lyo, C. N. Whang, J. Y. Won, and H. J. Kang, Appl. Phys. A: Mater. Sci. Process. **70**, 431 (2000).
[18] E. Budke, T. Surholt, S. Prokofjev, L. S. Shivndlerman, and C. Herzig, Acta Mater. **47**, 385 (1999).
[19] N. D. Browning, I. Arslan, P. Moeck, and T. Topuria, Phys. Status Solidi B **227**, 229 (2001).